Estimating *p-y* curves for clays by CPTU method: a framework and empirical study

Hongjiang Li

PhD Student, Jiangsu Key Laboratory of Urban Underground Engineering & Environmental Safety (Southeast University), Institute of Geotechnical Engineering, Nanjing, 210096, China. (lihongjiang55@126.com)

Songyu Liu

Professor, Jiangsu Key Laboratory of Urban Underground Engineering & Environmental Safety, (Southeast University), Institute of Geotechnical Engineering, Nanjing 210096, China. (liusy@seu.edu.cn)

Liyuan Tong

Professor, Jiangsu Key Laboratory of Urban Underground Engineering & Environmental Safety (Southeast University), Institute of Geotechnical Engineering, Nanjing, 210096, China. (atmu@seu.edu.cn)

Kangda Wang

PhD Student, School of Civil and Environmental Engineering, Nanyang Technological University, Blk N1, 50 Nanyang Avenue, 639798, Singapore. (729527503@qq.com)

Si Ha

Master Student, Jiangsu Key Laboratory of Urban Underground Engineering & Environmental Safety (Southeast University), Institute of Geotechnical Engineering, Nanjing, 210096, China. (1127021757@qq.com)

Submitted for publication in

International Journal of Geomechanics

Abstract: Despite its wide use as a tool in foundation design, the CPTU test was rarely recommended to work for design and analysis of laterally loaded piles. Obtaining lateral response of pile foundations is a complicated engineering problem, especially in nonhomogeneous soils. This paper presents a review of the relationship between the piezocone test and the bearing response of laterally loaded piles, and introduces a framework for estimating *p*-*y* curves for clays direct using CPTU parameters. In order to validate this method, full-scale lateral load tests of bored piles with corresponding CPTU tests in Jiangsu soil deposits were conducted and data were used for comparison with the predicted results. In addition, case histories were further considered in detail to study the application of the proposed method for different field conditions. It is demonstrated that the results predicted by the proposed CPTU-based *p*-*y* curve agree relatively well with the measured results. The proposed method can provide a fast and effective design tool that can be applied to clayey soils with full consideration of soil profiles along the pile embedded depth.

Key words: Piles; *p*-*y* curve; piezocone penetration test (CPTU); clays; load tests; case reports.

Introduction

Pile foundations are often required to be designed against significant lateral loads in addition to vertical loads. These lateral loads can be imposed by wind, earthquake, wave, earth pressure, etc. For the estimation of lateral load capacity of a single pile and the purpose of doing an efficient and safe pile foundation design, the pile-soil interaction characteristics should be evaluated accurately. However, the bearing capacity of laterally loaded piles is mainly controlled by the

forms of the lateral soil resistance. The non-linear and elastic-plastic response of surrounding soils as well as the non-homogeneity of soil properties makes the analysis of laterally loaded piles difficult and restricts development of the design methods.

In the determination of the bearing capacity of laterally loaded piles, well-known analytical theories and numerical methods have certain shortcomings. Furthermore, full-scale pile load tests are very expensive and time-consuming. Laboratory model tests disturb the soil and centrifuge tests have large energy consumption. All of these are challenging for engineers to effectively select an appropriate method. Therefore, to overcome the shortages of the traditional methods, a practical and fast method should be proposed to evaluate the lateral behavior of pile foundations.

Among various foundation design methods, the piezocone penetration test (CPTU) is adopted in soil investigation due to its cost-effectiveness and popularity (Robertson, 2009). For the design of laterally loaded piles, however, less attention and attempt were paid to the CPTU test mainly due to the different loading direction of the vertical cone penetration from the lateral pile loading process (Kim et al. 2014). Because of the simplicity of the beam-on-elastic foundation (BEF) approach (Ashour et al. 2004), the lateral pile-soil interaction behavior is commonly characterized by a series of uncoupled nonlinear springs which are applied along the pile embedded depth. These are known as *p-y* curves (Randolph et al. 2005; Taghavi and Muraleetharan 2016). Up to date, several formulations have been suggested to predict *p-y* curves in different soil conditions (Matlock 1970; Reese et al. 1975; Murchison and O'Neill 1984; Franke and Rollins 2013). Moreover, various commercial programs based on *p-y* analysis have been established to aid engineers in lateral load analysis (e.g. *LPILE* (Ensoft 1999), Com624P (Reese and Wang 1993), FloridaPier (FDOT, 1996), ALP program (Oasys 2013). All the programs

require inputs of soil parameters at different depths and the adequacy of input profiles is crucially important for the successful implementation of the *p-y* analysis.

This paper aims at describing the feasibility of estimating *p-y* curves by the CPTU method for analysis of laterally loaded piles in clays. A CPTU-based *p-y* analysis method is established to calculate the lateral load capacity and evaluate the lateral bearing characteristics of single piles, by building the relationship between Matlock *p-y* curve parameters and CPTU profiles. In order to examine the accuracy of the proposed method, field full-scale lateral pile test results in Jiangsu soil deposits were conducted and used for comparison with the predicted results.

Correlation between cone resistance and lateral pile load capacity

In-situ cone penetration tests (CPTs) having less average cost than traditional soil boring or corresponding laboratory and field tests are widely used in soil investigation, vertical bearing pile design and other geotechnical engineering issues (Puppala et al. 1995; Lunne et al. 1997; Mayne 2007; Liu et al. 2011; Cai et al. 2012; Shahin 2013). In recent years, a group of scientists began to focus on the application of CPT technique to the analysis of pile foundations under lateral loads. Some beneficial explorations have been undertaken and several studies are available for describing the potential correlation between cone resistance and pile lateral load capacity (Schnaid and Housby 1991; Anderson et al. 2003; Abu-Farsakh et al. 2003; Lee et al. 2010; Suryasentana and Lehane 2014; Bouafia 2014; Ebrahimian et al. 2015). It has been recognized that the cone resistance can be expressed as a function of the horizontal soil effective stress rather than the vertical soil effective stress, which is similar to the bearing mechanism of laterally loaded piles (Schnaid and Housby 1991; Lee et al. 2010). Moreover, a comprehensive comparison of four test

methods (SPT, CPT, DMT, and PMT) conducted by Anderson et al. (2003) also indicated that CPT has a prominent prediction accuracy in evaluating the bearing capacity of laterally loaded piles. A numerical derivation of a CPT-based *p-y* curve for piles was proposed previously by Suryasentana and Lehane (2014) for sands employing hardening soil (HS) models. However, there is still no theoretical explanation for that the cone resistance is mainly controlled by horizontal soil effective stress.

As an advanced technology, the CPTU test generally provides three separate measurement readings including the cone tip resistance q_c, sleeve frictional resistance f_s and penetration pore-water pressures u_2, and also gives nearly continuous information about the field subsurface stratification. Fig.1 shows physical and schematic diagrams of the international standard CPTU piezocone with a projected area of 1000 mm^2, an apex angle of 60º, and a sleeve surface area of 15000 mm^2 (Tong et al. 2011).

In the process of a CPTU test, along with continuous penetration of the probe (rate of 2 cm/s), plastic damage in soils will be produced near the cone tip. The cone tip resistance consists of two parts, the normal stress σ_n perpendicular to the cone tip side, and the shear stress τ along the cone tip wall (see Fig.1). The shear stress τ defined by Konrad and Roy (1987) is given as follows:

$$\tau = (\sigma_n - u_m) M \tan\phi' \quad (1)$$

where ϕ' is the internal soil friction angle, M is the contact surface friction coefficient, and u_m is the pore water pressure in the position of the plastic damage area, which is represented by:

$$u_m = \alpha u_2 \quad (2)$$

where u_2 is the penetration pore-water pressure at the shoulder position (see Fig.1), and α is the

conversion factor, range in 1 ~ 1.1(Roy et al. 1982). To obtain the corrected cone resistance for pore pressure effects, a correction must be applied to account for the design of the cone. The actual cone resistance q_t is obtained as follows (Campanela et al 1981; Liu et al. 2004):

(3) $$q_t = q_c + u_2(1-a)$$

where a is the bearing net area ratio, a=0.8.

The following expression for a cone with half apex angle θ and diameter d is then obtained considering the force equilibrium in the failure zone:

(4) $$q_t \cdot d = 2(\sigma_n \cdot \frac{d}{2\sin\theta} \cdot \sin\theta) + 2(\tau \cdot \frac{d}{2\sin\theta} \cdot \cos\theta)$$

From Eq. (1) and Eq. (2), the balance equation above can be simplified as follows:

(5) $$q_t = \sigma_n + (\sigma_n - \alpha u_2) M \tan\phi' \cot\theta$$

As indicated by Eq. (5) and Fig. 1, the actual total stress q_t is directly related to the normal stress σ_n. Here, the definition of horizontal soil effective stress σ_h and vertical soil effective stress σ_v is given, and σ_n can be decomposed by σ_h and σ_v as follows:

(6) $$\sigma_n = \sigma_h \cos\theta + \sigma_v \sin\theta$$

For standard CPTU cone, the apex angle is immobilized 60º and its half is θ=30° (see Fig.1). The contribution ratio of the σ_h and σ_v for the normal stress σ_n can be calculated by the ratio of $\cos\theta$ and $\sin\theta$, so that the result is obviously σ_h : σ_v =1.73:1 from a simple but persuasive analysis. That is to say, the CPTU cone resistance q_t is mainly controlled by the horizontal soil effective stress σ_h rather than the vertical soil effective stress σ_v, which is consistent with the previous conclusion (Schnaid and Housby 1991; Lee et al. 2010). For laterally loaded piles, it is well

135 known that the horizontal soil effective stress σ_h affects the level of the pile bearing performance,
136 indicating that estimation of lateral pile capacity using CPTU results is feasible.

137 Framework for constructing CPTU-based *p-y* curves

138 *Matlock (1970) p-y curve*

139 It is generally accepted that the *p-y* curve has a non-linear shape and is characterized by
140 certain soil parameters. For laterally loaded piles in clays, the *p-y* curve proposed by Matlock
141 (1970) is widely used and adopted in various specifications (API 2000; DNV 2004; JTS 2012).
142 Fig.2 shows the curve feature of the Matlock *p-y* model applying in soft clay. Soft clay is widely
143 distributed in China's coastal areas, especially in Jiangsu province (Liu et al. 2008). The function
144 of the Matlock *p-y* curve in Fig.2 is given in the following normalized form:

145 (7) $$\frac{p(z)}{p_u} = 0.5 \cdot [\frac{y(z)}{y_{50}}]^{1/3}$$

146 where $p(z)$ is the lateral load per unit length, p_u is the ultimate lateral soil resistance, $y(z)$ is the pile
147 lateral displacement and y_{50} is the critical lateral displacement. As shown in Fig.2, the $p(z)$ value is
148 set as a constant p_u beyond the lateral displacement of $8y_{50}$. Because of fewer parameters and
149 simple form, this *p-y* relation is widely adopted to the simulation of clays.

150 For the analysis of the ultimate lateral resistance of surrounding soils, p_u complies with the
151 following equation:

152 (8) $$p_u = N_c s_u D$$

153 where s_u is the undrained shear strength, D is the pile diameter and N_c is a bearing capacity factor.
154 According to Matlock (1970), N_c varies from 3 to 9 depending on the depth range given as

follows:

$$N_c = 3 + \frac{\gamma' z}{s_u} + \frac{0.5z}{D} \quad (z < z_r)$$
$$N_c = 9 \quad (z \geq z_r) \tag{9}$$

where γ' is the effective unit weight of soils, z is the depth from the ground surface and z_r is the limit depth below ground surface which can be estimated using the following relationship (Matlock, 1970):

$$z_r = \frac{6D}{\gamma' \frac{D}{s_u} + 0.5} \tag{10}$$

CPTU parameters for the derivation of Matlock *p-y* curve

Since current design software such as *LPILE* for estimating the lateral load capacity of piles commonly requires *p-y* curves, which originated from the Matlock *p-y* model for clays. This section presents the methodology to obtain the Matlock *p-y* curves from CPTU parameters. The corresponding comprehensive relationship between piezocone parameters and *p-y* curve parameters p_u, y_{50} is established, and the CPTU-based *p-y* analysis method for clays is proposed.

Ultimate lateral soil resistance p_u

Undrained shear strength s_u for clays as shown in Eq. (8), is one of the important characterization factors for determination of p_u values. An effective way to obtain the p_u is to use CPTU data to obtain the s_u firstly. The cone factor method is a common approach to estimate s_u using the CPTU cone resistance given as the following relationship:

$$s_u = \frac{q_t - \sigma_{v0}}{N_{kt}} \tag{11}$$

where N_{kt} is the cone factor, and σ_{v0} is the in situ total vertical stress. This method is simple to apply and accounts for the influence of stress level on soil strengths. As the parameter σ_{v0} cannot be obtained from the piezocone test, the rapidity and efficiency of CPTU technology are reduced. In order to overcome this defect, the effective cone factor method was proposed (Lee et al. 2010), and s_u can be defined by:

$$s_u = \frac{q_t - u_2}{N_e} = \frac{q_e}{N_e} \tag{12}$$

where q_e is the effective cone resistance, and N_e is the effective cone factor. Noted that no additional testing procedure is required as all parameters in Eq. (12) can be obtained from CPTU results. Substituting Eq. (12) into Eq. (8), the following equation can be obtained after rearranging:

$$p_u = \frac{N_c}{N_e} D q_e \tag{13}$$

Critical lateral displacement y_{50}

For critical lateral displacement y_{50}, according to API (1993), y_{50} is defined as follows:

$$y_{50} = 2.5 \varepsilon_{50} D \tag{14}$$

where D is the pile diameter and ε_{50} is the limit strain corresponding to 50% of failure stress in unconfined compression tests.

However, the parameter ε_{50} is particularly sensitive to the disturbance of soils in a laboratory. The ε_{50} value of remolded soils is different from the one of undisturbed soils. Instead, in-situ tests, such as DMT, PMT, and CPT/CPTU, can achieve minimum disturbance and provide more

192 accurate original soil parameters. Table 1 shows four equations for estimating ε_{50} (%) by
193 Ebrahimian et al. (2015) using CPT data. The Model 3 equation from Table 1 is presented as
194 follows:

195 (15) $$\varepsilon_{50} = 0.86 q_c - 0.5$$

196 Obviously, M3 has the highest accuracy with R^2=0.92 among the four models. Another
197 advantage is that Eq.(15) can predict ε_{50} more directly requiring only one parameter q_c. Therefore,
198 in this study Eq.(15) is adopted to determine the y_{50} of the Matlock *p-y* curve through Eq. (14). In
199 order to achieve dimensionless of ε_{50} values, the Eq.(15) is rewritten as the following form.

200 (16) $$\varepsilon_{50} = 0.086 \frac{q_c}{p_a} - 0.5$$

201 In which p_a is the reference pressure, taken to equal atmospheric pressure (0.1MPa). The
202 units for q_c and p_a are in MPa. The Matlock *p-y* curve can be given from CPTU data combined
203 Eqs.(13) and (16). Specifically, the CPTU-based Matlock *p-y* curve is defined as:

204 (17) $$p(z) = 0.5\left(\frac{N_c}{N_e} q_e D\right)\left[\frac{100 y(z)}{(0.215 q_c / p_a - 1.25) D}\right]^{1/3}$$

205 Thus, it is appropriate to establish a framework for estimating *p-y* curves by CPTU data for
206 clays. The proposed CPTU-based *p-y* curve (Eq. (17)) can directly be imported into commercial
207 programs (e.g. *LPILE*), and the aim of fast calculation of lateral load capacity for pile design is
208 achieved. As the horizontal bearing capacity of a pile is mainly controlled by the upper soil layers,
209 a CPTU penetration depth of more than 20*D* (*D* designates pile diameter) in this study is
210 prescribed to satisfy the computational requirement. The different steps of illustrating the
211 application of the CPTU- based *p-y* analysis method are shown in Fig. 3. This method is quick and

212 efficient.

213 ## Verification of the method

214 ### Field test

215 In this section, field full-scale lateral pile tests with corresponding CPTU tests are conducted
216 and used to validate the proposed CPTU-based *p-y* model. Selected CPTU test sites are all
217 sensitive Quaternary deposits in Jiangsu Province of eastern China. These Quaternary deposits are
218 located in cities of Jingjiang and Kunshan (Fig. 4), and layered clays are mainly distributed. The
219 test piles in two sites belong to cast-in-place bored piles with slurry wall protection. The basic
220 parameters of the test piles are shown in Table 2. The CPTU test position is close to the center
221 position of the test pile along the opposite side of the loading direction. The distance between the
222 test pile and its adjacent CPTU hole is within 3m. A loading/unloading method is used for
223 conducting lateral pile load tests. The pile-head lateral load is applied in steps of 10% of the
224 ultimate lateral bearing capacity of the test piles. Prior to lateral load tests, a series of strain
225 gauges are first attached to the steel cage and then lowered into drill holes at Jingjiang site. In
226 detail, 30 pairs of strain gauges are distributed on the upper pile at a vertical interval of 1 m, and
227 10 pairs are distributed along the lower half of the pile at a vertical interval of 2 m. Fig. 5 shows a
228 schematic of the lateral pile load test set-up and the field data collection during the test process.

229 The piezocone penetration device used in this test is produced by Vertek-Hogentogler & Co.
230 of USA. The equipment is a versatile piezocone system equipped with advanced digital cone
231 penetrometers fitted with 60 ° tapered and 10 cm^2 tip area cones, which can provide the
232 measurement of cone tip resistance q_t, sleeve friction f_s, and penetration pore-water pressure u_2.

All the CPTU tests are conducted in accordance with international standards (ISSMFE 1989; ASTM D5778 2012) after the construction of piles. The groundwater table (GWT) at the test locations is documented immediately after the CPTU tests. The layer numbers and representative profiles of the CPTU soundings in two test sites are presented in Fig. 6. Required parameters (e.g., q_t, u_2, q_e) of the CPTU-based *p*-*y* curve (Eq. (17)) can be obtained directly from the piezocone penetration profiles. In Fig. 6, the u_0 line represents the hydrostatic pressure line.

Presentation and discussion of results

The bending moments of testing piles at every loading step are calculated by strain gauges, from which the soil reaction per unit length can be obtained (Kim et al. 2004). In this study, the measured bending moment is fitted as a seventh order polynomial function of *z* by the least-squares fitting method. By double differentiation and integration of the bending moments, the *p*-*y* curves at different depths are obtained (Zhu et al. 2012). The representative *p*-*y* curves of silty clay (layer No.①) and soft clay (layer No.②) derived from Eq. (17) at Jingjiang site in comparison with those of lateral pile load tests are depicted in Fig. 7. The soil resistance values of soft clay play out using half of the coordinate value (*p*/2) in the figure. It can be concluded that the predicted *p*-*y* curves from the proposed method agree well with that obtained from full-scale lateral load tests of instrumented piles. In addition, the lateral soil resistance values for silty clay show a reasonable increase from 1*D* to 4*D* (*D* means pile diameter) and are larger than that of soft clay.

The accuracy of the predicted allowable pile capacity (H_a) is checked by using Eq. (17) directly in *LPILE* program and then comparing the predicted results with that measured from

lateral load pile tests. For the determination of H_a, the load-deflection criterion given by JGJ 94-2008, *Chinese technical code for testing pile foundations* is adopted. A representative H-$\Delta Y/\Delta H$ curve for Jingjiang load test is shown in Fig. 8, where ΔY represents the horizontal displacement gradient of the pile head, and the value corresponding to the end of the first line is the allowable lateral pile capacity. Fig. 9 presents the H_a values obtained from the proposed method and the lateral load tests at Jingjiang and Kunshan sites. It can be concluded that the predicted and measured results are generally consistent considering the data scatter. The upper and lower bound lines in Fig. 9 show the boundaries of a zone, characterized by certain ratios of predicted values to measured values of H_a. The proposed CPTU-based *p-y* method in this study has a great advantage in predicting the horizontal bearing capacity of pile foundations with a (0.85-1.14) ratio boundary. The proposed method can give virtually the same H_a values as those from full-scale lateral pile load tests.

Application: Case history evaluation of lateral load pile responses

In order to further highlight and broaden the applicability of the proposed CPTU-based *p-y* method, the case study of lateral responses of bored piles using this method is performed. The two case histories are as follows.

1. Test piles in Yangtze River clay deposit at Jingjiang, Taizhou, China.

2. Test piles in Taihu Lake clay deposit at Wujiang, Suzhou, China.

The distribution and geologic formation of these two sites are shown in Fig. 4. Two bored piles called T1 and T2 in each site are installed and tested. A series of CPTU tests are performed nearby the position of test piles after the construction of piles and stress stability of surrounding

soils. In order to evaluate the proposed method, the *p-y* curves are derived at depth intervals of *D*/2 for every site from the CPTU profiles. Thereafter, the scale effect of laterally loaded piles (for Case 1) and the lateral pile response to the thickness variations of a very soft clay interlayer (for Case 2) are analyzed particularly.

Case 1: Test piles at Jingjiang

This case history involves large diameter and super-long bored piles with a diameter and length equal to 1.0m and 68m, respectively. The flexural rigidity of the pile body is EI $=0.16\times10^7$kN·m^2. The soil profiles at the test site show a composite soil layer condition with silty clay, soft clay, and some sand layers. CPTU tests adjacent to the test pile are conducted with a penetration depth reaching 33 m (33*D*). The typical profiles of q_t, u_2 and q_e with depth are presented in Fig. 6(a). Through inputting the *p-y* curves from Eq.(17) into *LPILE* program, a numerical model of the large diameter and super-long pile is established. The model's sketch and soil distribution are shown in Fig. 10, where the upper 33m clay layers adopt the CPTU-based *p-y* curves, while the underneath sand layers adopt build-in Reese's *p-y* curves of *LPILE* program.

Fig.11 shows the comparison of the measured and predicted lateral loaded-deflection (*H-Y*) curves and the bending moment (*M*) curves under H_a=172 kN of test piles (T1 and T2). The determination of H_a still adopts the method given by JGJ 94-2008, *Chinese technical code for testing pile foundations.* As shown in Fig. 11, the predicted results using CPTU-based *p-y* method are in close agreement with the field measured results. The maximum bending moment of the pile in this study occurs at (3 ～ 5) *D* depth below ground level. Owing to the accuracy of the CPTU-based *p-y* model in the *LPILE* program, the horizontal bearing response of the pile against

different pile diameters are further analyzed. Fig. 12 presents the calculated results of the piles with different diameters of 0.6*D*, 0.8*D*, 1.0*D*, 1.2*D*, 1.5*D*, 2.0*D*. It can be seen that the pile diameter has a significant impact on the bearing capacity of laterally loaded piles. The allowable bearing capacity increases with the increase of pile diameter. Taking the lateral load corresponding to 6 mm displacement as the design value of lateral pile capacities (JGJ 94-2008, *Chinese technical code for testing pile foundations*), the design value of 2.0*D* pile is 320kN, three times as much as that of 0.6 *D* pile. Additionally, the scale effect can change the stress distribution of deep pile bodies. With the increase of pile diameter, the bending moment grows, but the depth of maximum and zero bending moment positions reduce. These result in the increase of the horizontal bearing capacity of pile foundations.

Case 2: Test piles at Wujiang

This case history involves the lateral pile response to the thickness variations of a very soft clay interlayer in Taihu Lake site. The diameter, length and flexural rigidity of the bored pile are 0.7m, 55m, and EI =4.03×10^{5}kN·m^2, respectively. The previous survey determines that a soft clay interlayer with a thickness between (0.50 ~ 6.00) m is widely distributed overlying a clay layer. In-situ CPTU results based on Liu's China-soil classification chart (Liu et al. 2013), presented in Fig. 13, also show the existence of the very soft clay in the test field. A representative profile of piezocone penetration is shown in Fig. 14. For analysis of piles in Wujiang site, the predictive capability of the proposed *p-y* method is demonstrated beforehand by comparing predicted load-deflection curves and bending moment curves to the measured. As indicated by Fig. 15, the feasibility of the proposed *p-y* method is proven. Hence, the further analysis of lateral pile responses to the thickness variations of the soft clay interlayer can be conducted decisively.

Fig. 16 shows the comparison of the bending moment and the displacement for various soft clay interlayer thicknesses (h) under a given horizontal force H_a=150kN. Five thicknesses in this study are set: h=0.5m, 2.0m, 3.0m, 4.5m, 6.0m. For the bending moment distribution, although there is no change in the curve shape, the locations of maximum and zero bending moment positions move down, and the maximum bending moment values increase with the increase of interlayer thickness. The location and magnitude of the maximum bending moment, in this case, moves down by 85% and increases by 100%, respectively. The pile head displacement for h=6.0m is nearly four times larger than that for h=0.5m in this case. It can be concluded that the soft clay interlayer has a significant effect on the lateral bearing capacity of the piles. In addition, the increase rates of the maximum bending moment (M_{max}) and the pile head displacement (Y) are both reduced with the increase of interlayer thickness, and the M_{max}-h and Y-h curves flatten out after h=4.5m shown in Fig. 16. Those mean that the very soft clay interlayer within the scope of 4.5 m thickness is a key object for the lateral pile bearing capacity. If it exceeds 4.5m, the interlayer effect can be ignored, which can simplify the soil investigation for the pile design in the Taihu Lake area.

Conclusions

Obtaining the lateral response of pile foundations is a complicated engineering problem. Efforts have been made in this study to estimate p-y curves for clays by CPTU method. Case examples of lateral pile projects in Jiangsu soil deposits are executed to validate the proposed method. Based on the results, the following conclusions can be drawn:

(1) A CPTU-based p-y analysis method for estimating the lateral response of pile foundations is

proposed based on the relationship between CPTU profiles and Matlock *p-y* curve parameters. The proposed *p-y* model is convenient for the design of pile foundations, completely relying upon in-situ soil parameters.

(2) The predicted *p-y* curves direct from CPTU results agree well with that obtained from the full-scale lateral pile tests in this study. The allowable lateral capacity of the test bored piles obtained from the proposed method is consistent with that from field tests in Jiangsu soil deposits.

(3) Two cases are examined to broaden the applicability of the proposed CPTU-based *p-y* method for predicting the lateral pile responses in different clay sites. The scale effect of large diameter piles and the lateral pile response to thickness variations of the soft clay interlayer are examined.

(4) The CPTU-based *p-y* model is an efficient and rapid method for determining the bearing characteristics of laterally loaded piles in clays and can be used as an alternative to conventional methods. Further research with different soils and pile types (e.g. driven piles) should be carried out to improve the applicability of the model.

Acknowledgments

Great appreciation goes to the editorial board and the reviewers of this paper. Majority of the work presented in this paper was funded by the National Key R&D Program of China (Grant No. 2016YFC0800201), the National Natural Science Foundation of China (Grant No. 41572273), the Construction Science and Technology Research Project of Jiangsu Province (Grant No. 2014ZD66), and the Graduate Student Scientific Research Innovation Program of Jiangsu Province (KYLX16_0244). These financial supports are gratefully acknowledged.

References

362 Abu-Farsakh, M., Tumay, M., and Voyiadjis, G. 2003. Numerical parametric study of piezocone penetration test
363 in clays. International Journal of Geomechanics, 3(2), 170-181.

364 Anderson, J.B., Townsend, F. C., and Grajales, B. 2003. Case history evaluation of laterally loaded piles.
365 Journal of geotechnical and geoenvironmental engineering, 129(3): 187-196.

366 API. 2000. Recommended Practice for Planning, Designing and Construction Fixed Offshore
367 Platforms-Working Stress Design, American Petroleum Institute, API Recommended Practice 2A-WSD
368 (RP2AWSD),(21st Edition), Dallas, TX, USA.

369 Ashour, M., Pilling, P., and Norris, G. 2004. Lateral behavior of pile groups in layered soils. Journal of
370 Geotechnical and Geoenvironmental Engineering, 130(6), 580-592.

371 ASTM D5778, 2012. International Standard Test Method for Electronic Friction Cone and Piezocone
372 Penetration Testing of Soils, Annual Book of ASTM Standards. ASTM International, West Conshohocken,
373 PA.

374 Bouafia, A. 2014. P-Y curves from the CPT test for laterally loaded single piles in sand. In Proceedings of 3rd
375 international symposium on cone penetration testing, Las Vegas, Nevada, USA.

376 Broms B B. 1964. Lateral resistance of piles in cohesionless soils. Journal of the Soil Mechanics and
377 Foundations Division, 90(3): 123-158.

378 Cai, G., Liu, S., and Puppala, A.J. 2012. Reliability assessment of CPTU-based pile capacity predictions in soft
379 clay deposits. Engineering Geology, 141, 84-91.

380 Campanella, R.G., Gillespie, D.G., and Robertson, P.K. 1981. Pore pressures during cone penetration testing.
381 Department of Civil Engineering, University of British Columbia.

382 DNV. 2004. Det Norske Veritas, Design of Offshore Wind Turbine Structures, Offshore Standard, Norway.

383 Ebrahimian, B., Nazari, A. and Pasha, A. Y. 2015. Evaluating ε50 for lateral load–displacement behavior of piles
384 in clay. Ocean Engineering, 96: 149-160.

385 Ensoft, Inc. 1999. LPILE Plus 3 for Windows—A program for the analysis of piles and drilled shafts under
386 lateral loads, (http://www.ensoft.com).

387 Florida Department of Transportation (FDOT). 1996. FloridaPier users manual,
388 (http://www.dot.state.fl.us/structures/proglib.htm).

389 Franke, K. and Rollins, K. 2013. Simplified hybrid p-y spring model for liquefied soils. J. Geotech. Geoenviron.
390 Eng., ASCE, 139(4), 564-576.

391 ISSMFE, 1989. International reference test procedure for cone penetration test (CPT). Report of the ISSMFE
392 Technical Committee on Penetration Testing of Soils-TC 16, with Reference to Test Procedures 7. Swedish
393 Geotechnical Institute, Linköping, Information, pp. 6-16.

394 JGJ 94-2008. Chines technical code for testing pile foundations. Beijing: China Building Industry Press, 2008.

JTS. 2012. Code for pile foundation of Harbor engineering. Ministry of transport, China.

Kim, G., Park, D., Kyung, D., and Lee, J. 2014. CPT-based lateral displacement analysis using p-y method for offshore mono-piles in clays. Geomechanics and Engineering, 7(4), 459-475.

Konrad, J. M., and Roy, M. 1987. Bearing capacity of friction piles in marine clay. Geotechnique, 37(2), 163-175.

Lee J. 2013. Erratum for "Estimation of Lateral Load Capacity of Rigid Short Piles in Sands Using CPT Results" by Junhwan Lee, Minki Kim, and Doohyun Kyung. Journal of Geotechnical and Geoenvironmental Engineering, 139(6): 1005-1005.

Lee, J., Kim, M., and Kyung, D. 2010. Estimation of lateral load capacity of rigid short piles in sands using CPT results. J. Geotech. Geoenviron. Eng., ASCE, 136(1), 48-56.

Liu, S.Y., Cai, G.J., Puppala, A.J., and Tu, Q.Z. 2011. Prediction of embankment settlements over marine clay using piezocone penetration tests. Bull. Eng. Geol. Environ. 70 (3), 401–409.

Liu, S.Y., Cai, G.J., Tong, L.Y., and Du, G.Y. 2008. Approach on the engineering properties of Lianyungang marine clay from piezocone penetration tests. Marine Georesources and Geotechnology, 26(3), 189-210.

Liu, S.Y., Cai G.J., and Zou H.F. 2013. Practical soil classification methods in China based on piezocone penetration tests. Chinese Journal of Geotechnical Engineering, 35(10): 1765-1776.

Liu, S.Y. and Wu, Y.K. 2004. On the strategy and development of CPT in China. Chinese Journal of Geotechnical Engineering, 26(4): 553–556.

Lunne, T., Robertson, P.K., and Powell, J.J.M. 1997. Cone penetration testing in geotechnical practice. Blackie Academic and Professional.

Matlock, H. 1970. Correlations for design of laterally loaded piles in soft clay. Proc. 2nd Offshore Tech. Conf., Houston, Texas 1, 577-594.

Mayne, P.W., 2007. Cone penetration testing: a synthesis of highway practice. NCHRP Synthesis 368. Transportation Research Board, National Academies Press, Washington, D.C.

Murchison, J.M. and O'Neill, M.W. 1984. Evaluation of p-y relationships in cohesionless soils. Anal. Des. Pile Found., ASCE, 174-191.

O'Neill, M. W., and Gazioglu, S. M. 1984. Evaluation of p-y relationships in cohesive soils. Proc., Analysis and Design of Pile Foundations, ASCE Technical Council on Codes and Standards, ASCE National Convention, J. Meyers, ed., New York, 192-213.

Oasys. 2013. Geotechnical Software., ALP manual, www.oasys-software.com, UK.

Puppala, A.J., Acar, Y.B., and Tumay, M.T. 1995. Cone penetration in very weakly cemented sand. J. Geotech. Eng. 121 (8), 589–600.

Randolph, M., Cassidy, M., Gourvenec, S., and Erbrich, C. 2005. Challenges of offshore geotechnical

engineering. In Proceedings of the international conference on soil mechanics and geotechnical engineering, 16(1), 124-176.

Reese, L.C., Cox, W.R., and Koop, F.D. 1975. Field testing and analysis of laterally loaded piles in stiff clay. Proc., 7th Offshore Technology Conf., Paper No. OTC 2312, 672–690.

Reese, L.C., and Wang, S. 1993. Com624P-Laterally loaded pile analysis program for the microcomputer, version 2.0. U.S. DOT Publication No. FHWA-SA-91-048, Washington, D.C.

Reese, L.C., and Welch, R.C. 1975. Lateral loading of deep foundations in stiff clay. J. Geotech. Eng. Div., Am. Soc. Civ. Eng., 101(7), 633–694.

Robertson P K. 2009. Interpretation of cone penetration tests-a unified approach. Canadian Geotechnical Journal, 46(11): 1337-1355.

Roy, M., Tremblay, M., Tavenas, F., and Rochelle, P. L. 1982. Development of pore pressures in quasi-static penetration tests in sensitive clay. Canadian Geotechnical Journal, 19(2), 124-138.

Schnaid, F., Houlsby, G.T. 1991. Assessment of chamber size effects in the calibration of in situ tests in sand. Geotechnique, 41(3): 437-445.

Shahin, M. A. 2013. Load–Settlement Modeling of Axially Loaded Drilled Shafts Using CPT-Based Recurrent Neural Networks. International Journal of Geomechanics, 14(6), 06014012.

Suryasentana, S.K., Lehane, B.M. 2014. Numerical derivation of CPT-based p-y curves for piles in sand. Géotechnique-, 64(3): 186-194.

Taghavi, A., and Muraleetharan, K. K. 2016. Analysis of laterally loaded pile groups in improved soft clay. International Journal of Geomechanics, 17(4), 04016098.

The Professional Standards Compilation Group of People's Republic of China. 2008. JGJ 94-2008 Technical code for building pile foundation. Beijing: China Architecture and Building Press.

Tong, L., Wang, Q., Du, G., Liu, S., and Cai, G. 2011. Determination of undrained shear strength using piezocone penetration test in clayey soil for bridge foundation. Journal of Southeast University, 27(2), 201-205.

Welch, R.C., and Reese, L.C. 1972. Lateral load behavior of drilled shafts. Research Rep. No. 3-5-65-99, conducted for Texas Highway Department and U.S. Department of Transportation, Federal Highway Administration, Bureau of Public Roads, Center for Highway Research, Univ. of Texas at Austin, Tex.

Zaaijer, M.B. 2006. Foundation modelling to assess dynamic behavior of offshore wind turbines. Applied Ocean Research, 28(1), 45-57.

Zhang, L.Y., and Chen, Z.C. 1992. A new p-y curve construction method in cohesive soils. Journal of the ocean engineering, 10 (4):50-58.

Zhang L.Y., Silva F, and Grismala R. 2005. Ultimate lateral resistance to piles in cohesionless soils. Journal of Geotechnical and Geoenvironmental Engineering, 131(1): 78-83.

Zhu, B., Chen, R.P., Guo, J.F., Kong, L.G., and Chen, Y.M. 2011. Large-scale modeling and theoretical investigation of lateral collisions on elevated piles. Journal of Geotechnical and Geoenvironmental Engineering, 138(4), 461-471.

List of Tables

Table 1 Models to determine ε_{50} (Ebrahimian et al. 2015)

Model	Equation	Parameter	R^2(%)
M1	$\varepsilon_{50} = 16.3 s_u - 0.7$	s_u	74.9
M2	$\varepsilon_{50} = 5 s_u OCR - s_u - 0.01 OCR - 0.5$	s_u, OCR	81.4
M3	$\varepsilon_{50} = 0.86 q_c - 0.5$	q_c	91.7
M4	$\varepsilon_{50} = 0.85 q_{net} + 0.1$	q_{net}	85.8

Note: Net cone tip resistance $q_{net} = q_{c+} u_2 (1-\alpha)-\sigma_{vo}$; R^2 is the correlation coefficient, and the higher the value is, the greater the precision.

Table 2 Characteristics of investigated piles

Test site	Pile type	Length /m	Diameter /mm	Allowable horizontal bearing capacity /kN
Jingjiang	Bored pile	68	1000	172
Kunshan	Bored pile	47	700	135

List of Figures

504 *p-y* curves at Jingjiang site

505 **Fig. 8** Determination of H_a value from the H-$\Delta Y/\Delta H$ curve

506 **Fig. 9** Comparison of predicted and measured H_a values for test piles at Kunshan and Jingjiang
507 sites

508 **Fig. 10** Schematic of the *LPILE* numerical model based on the proposed *p-y* curves

509 **Fig. 11** Comparison of measured and predicted (a) pile head deflections and (b) bending moments
510 under H_a=172kN

511 **Fig. 12** Responses for various diameter piles: (a) lateral loaded-deflection curves; (b) bending
512 moment curves under H_a=172kN

513 **Fig. 13** Soil behavior type classification chart from CPTU data based on Liu's method at Wujiang
514 site

515 **Fig. 14** Representative profiles of piezocone penetration test at Wujiang site

516 **Fig. 15** Comparison of numerical predictions with field measurements: (a) lateral
517 loaded-deflection curves; (b) bending moment curves.

518 **Fig. 16** Responses of piles subjected to H_a=150kN for various soft clay interlayer thicknesses: (a)
519 bending movements; (b) lateral pile deflections; (c) maximum bending moments; (d) pile head
520 displacements

521

522

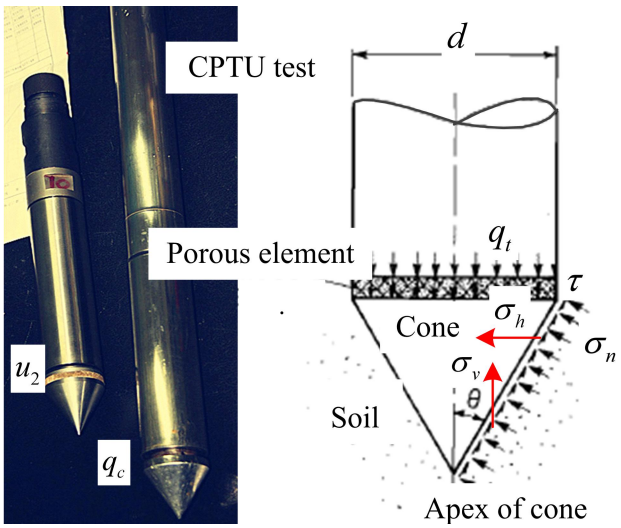

Fig. 1 Physical and schematic diagrams of a piezocone penetrometer

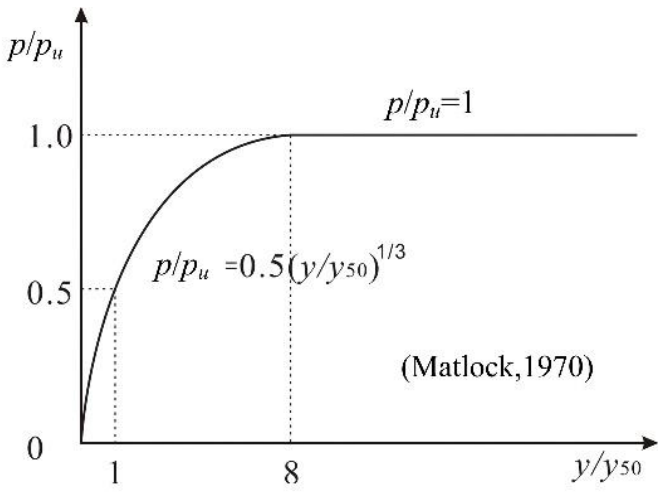

Fig. 2 Schematic shape of Matlock (1970) *p-y* curve

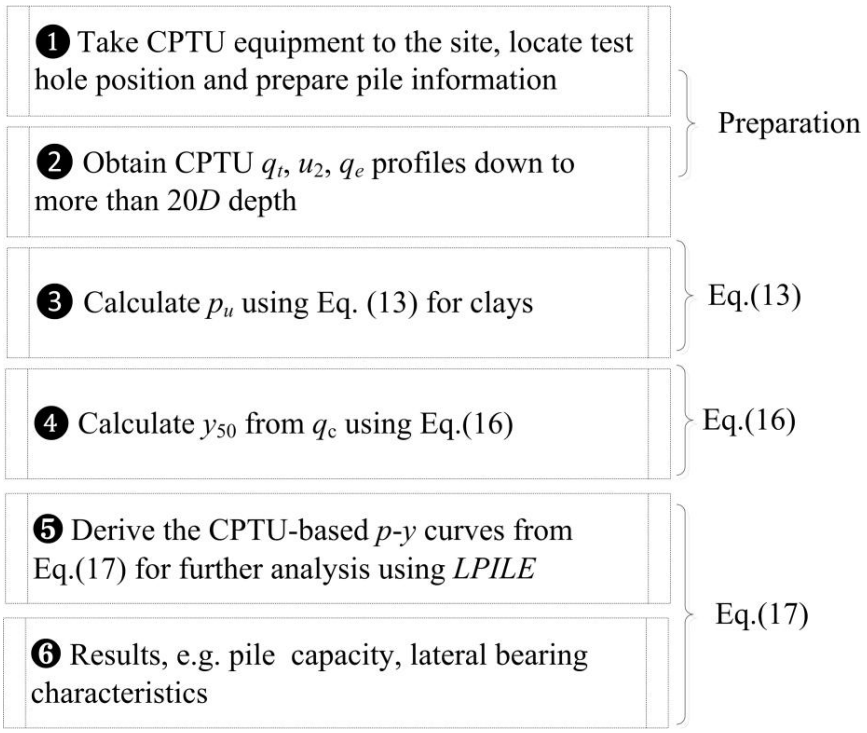

Fig. 3 Step-by-step application of the CPTU-based p-y analysis method

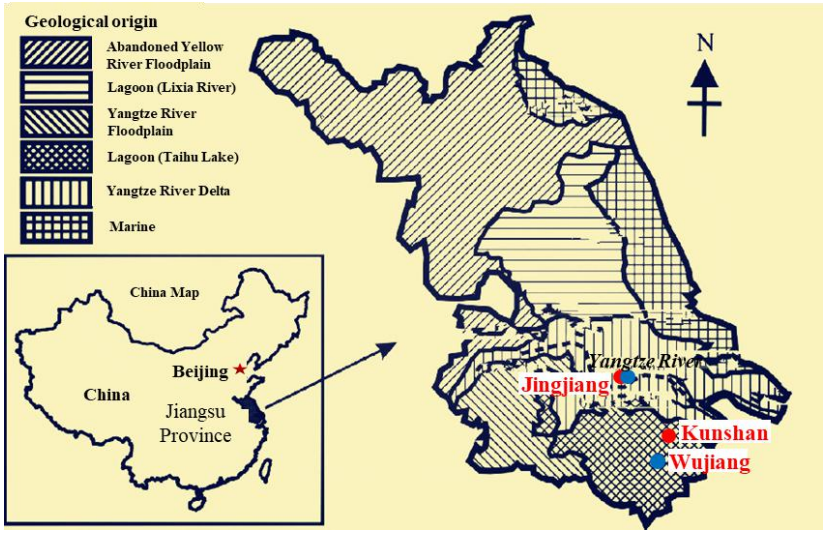

Fig. 4 Distribution and geologic formation of the testing sites

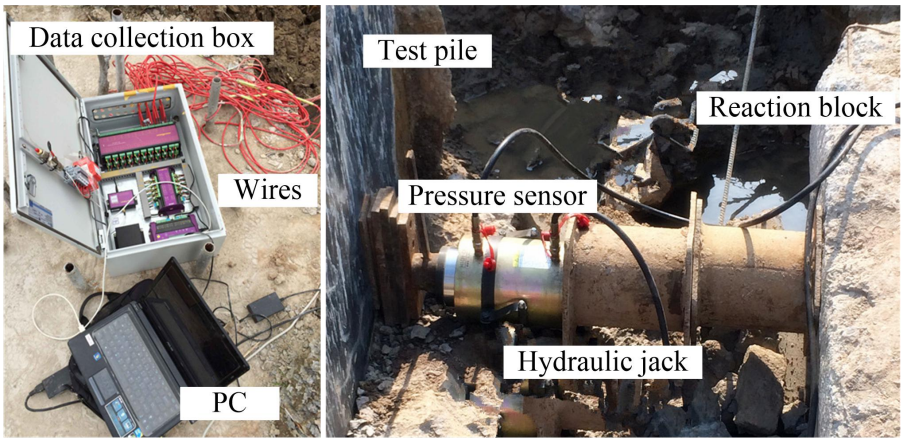

Fig. 5 Photos of lateral pile load test set-up and field data collection

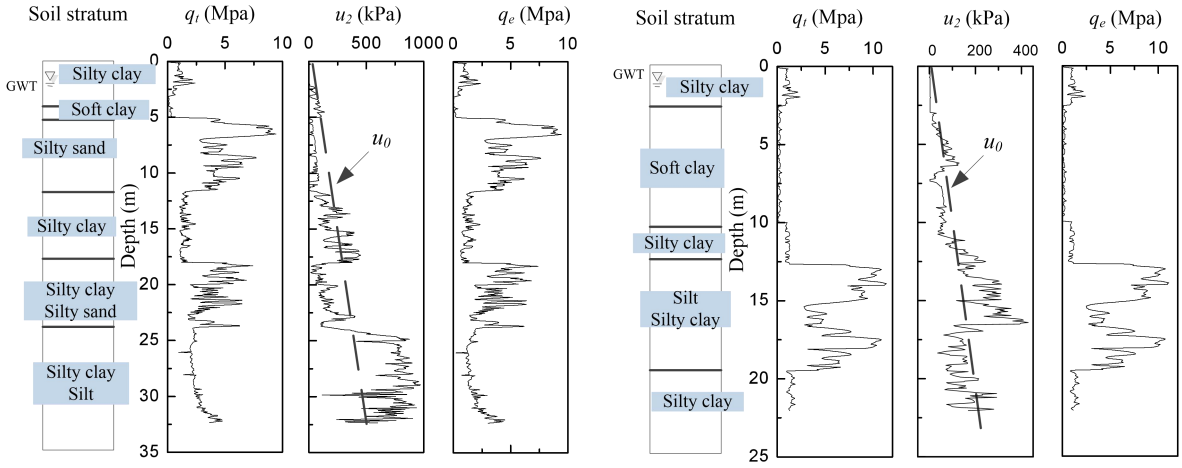

Fig. 6 Representative profiles of piezocone penetration tests: (a) Jingjiang site (layer No.①～⑥); (b) Kunshan site (layer No.①～⑤)

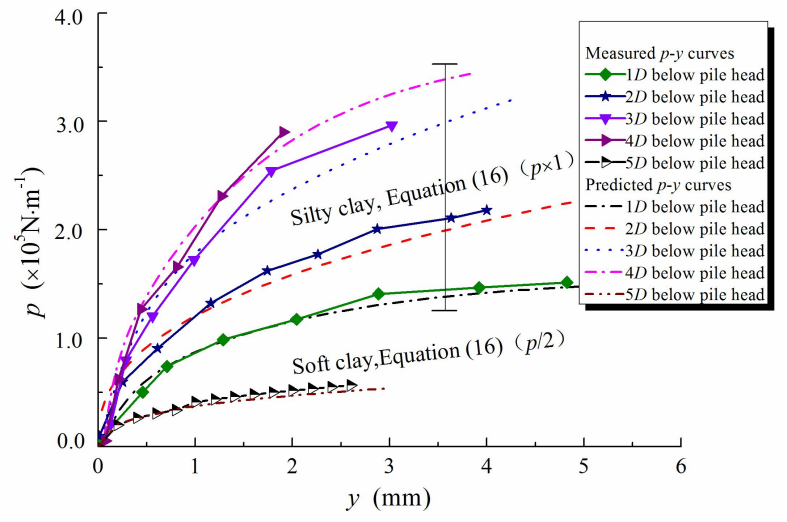

Fig. 7 Comparison of predicted (from CPTU data) and measured (from moments in pile section) *p*-*y* curves at Jingjiang site

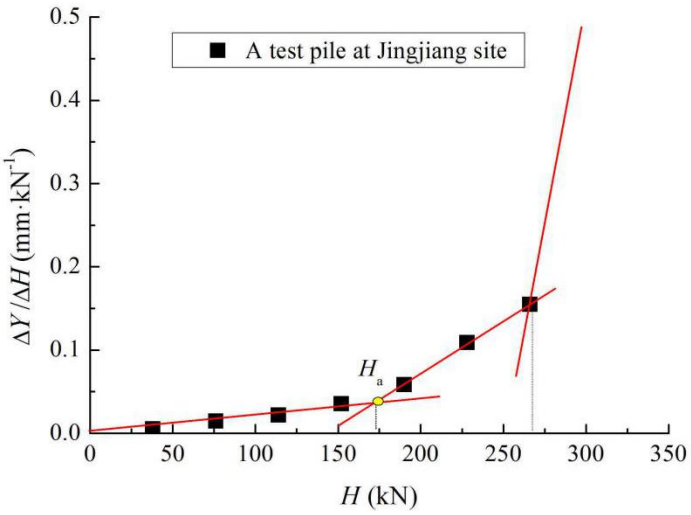

586

587 **Fig. 8** Determination of H_a value from the H-$\Delta Y/\Delta H$ curve

588

589

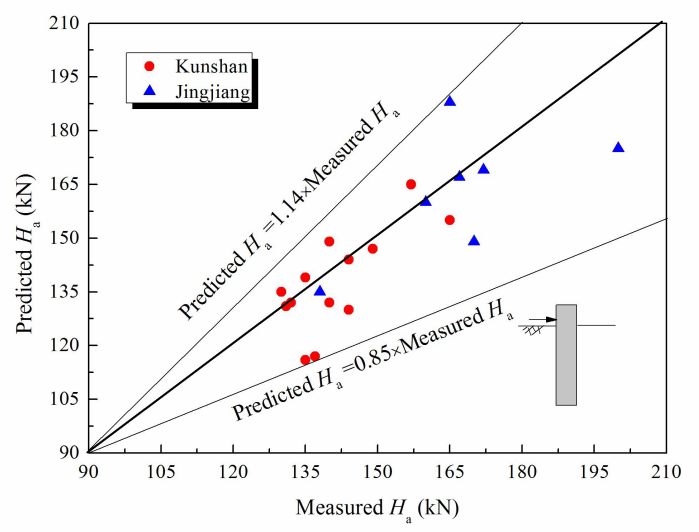

590

591

592 **Fig. 9** Comparison of predicted and measured H_a values for test piles at Kunshan and
593 Jingjiang sites

594

595

596

597

598

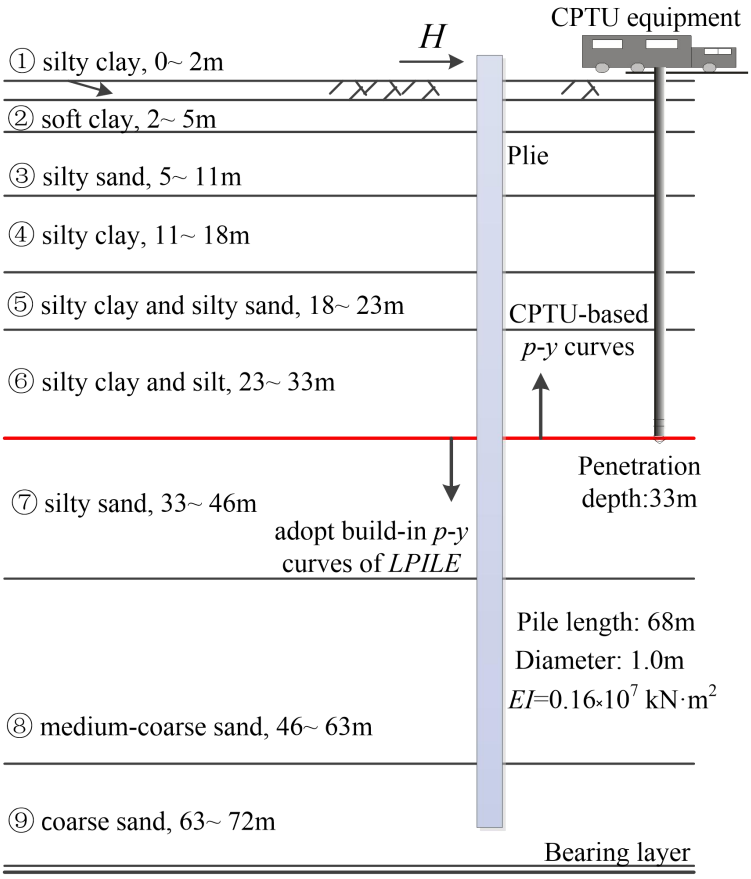

Fig. 10 Schematic of the *LPILE* numerical model based on the proposed *p-y* curves

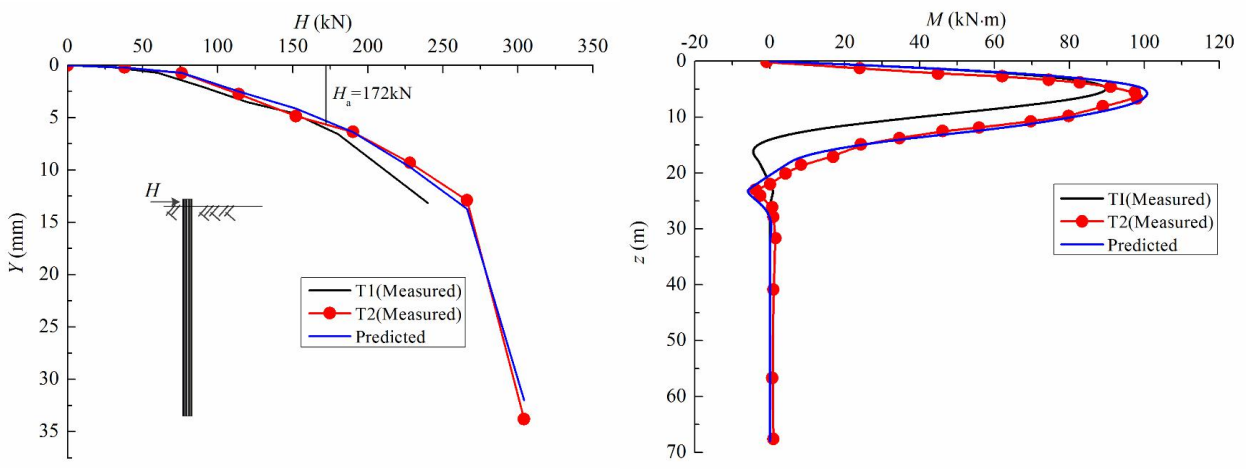

(a) (b)

Fig. 11 Comparison of measured and predicted (a) pile head deflections and (b) bending moments under H_a=172kN

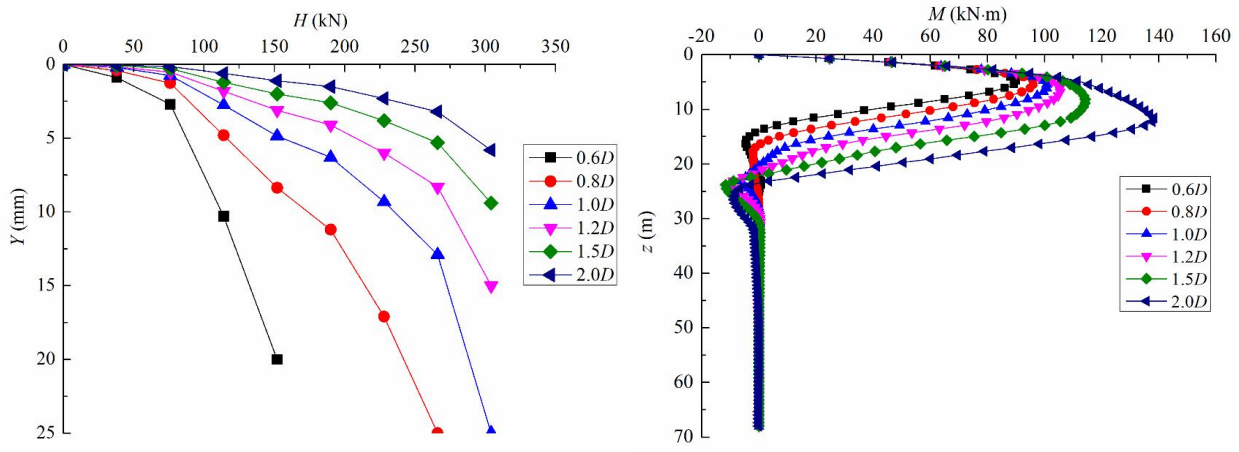

(a) (b)

Fig. 12 Responses for various diameter piles: (a) lateral loaded-deflection curves; (b) bending moment curves under H_a=172kN

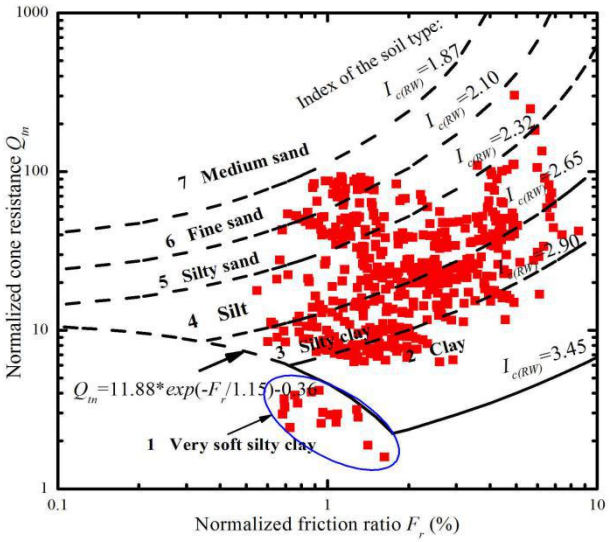

Fig. 13 Soil behavior type classification chart from CPTU data based on Liu's method at Wujiang site

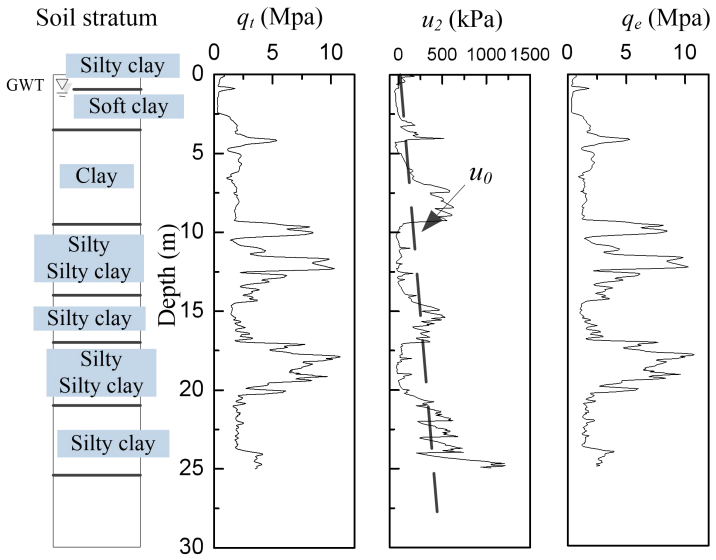

Fig. 14 Representative profiles of piezocone penetration test at Wujiang site

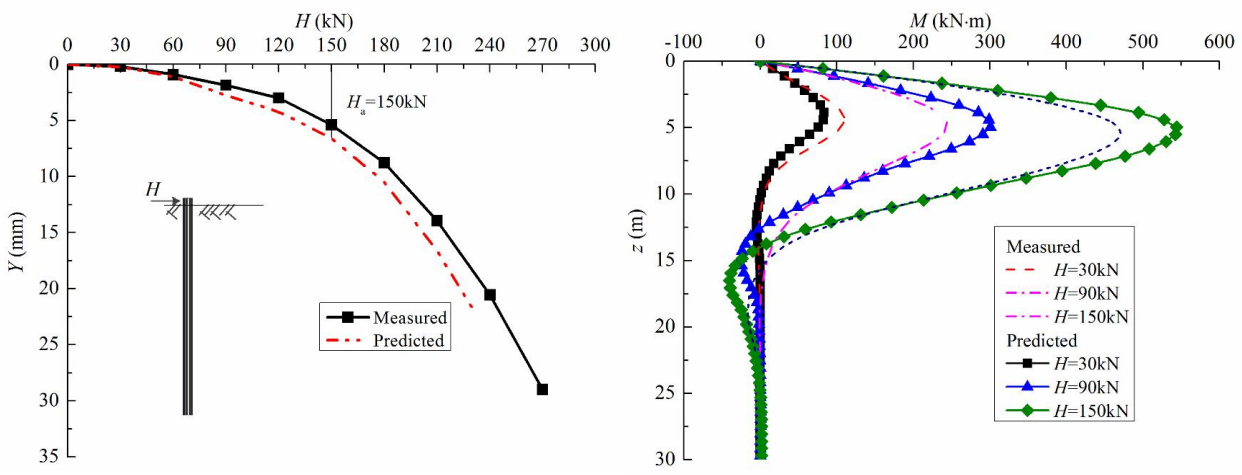

(a) (b)

Fig. 15 Comparison of numerical predictions with field measurements: (a) lateral loaded-deflection curves; (b) bending moment curves.

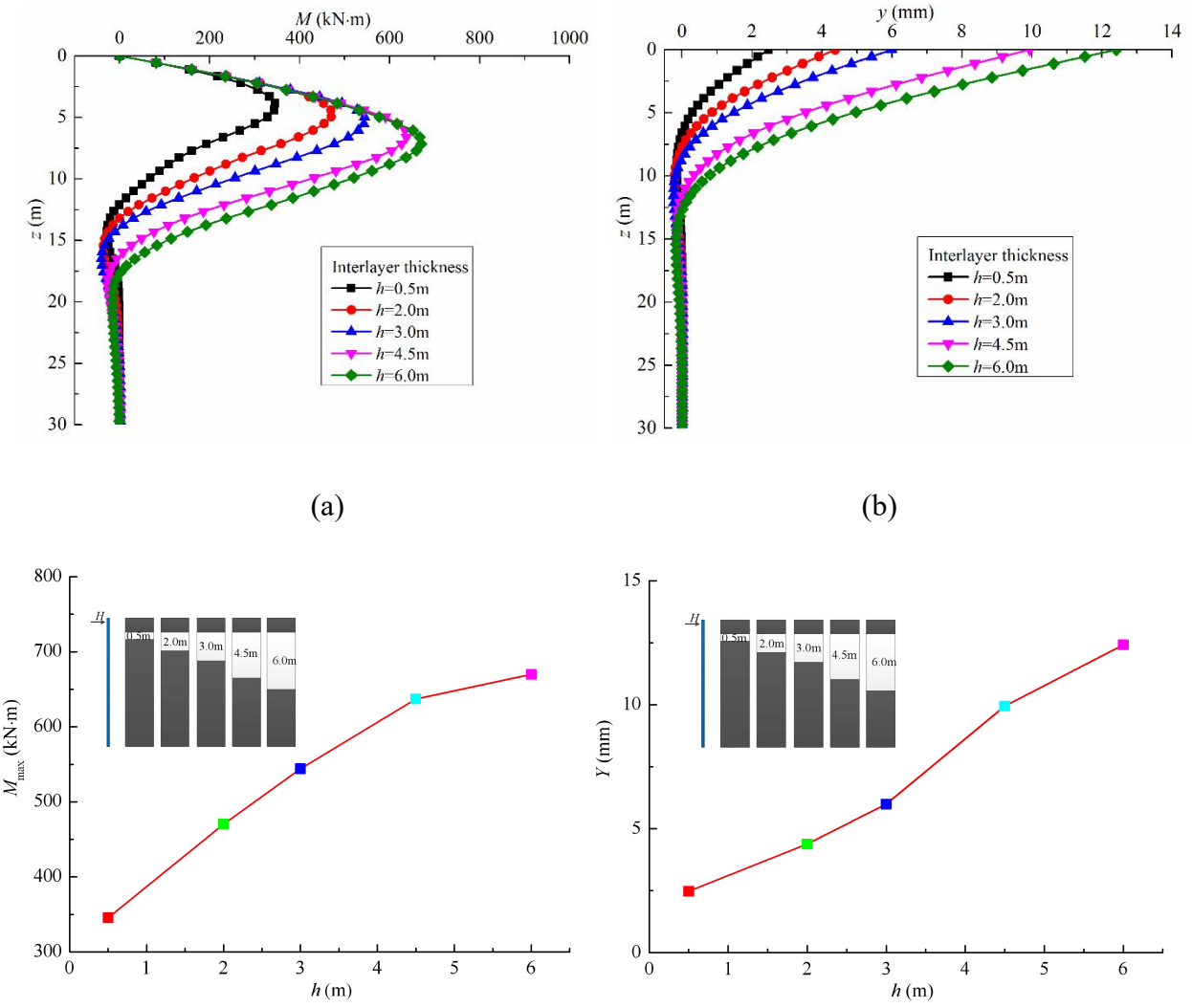

Fig. 16 Responses of piles subjected to H_a=150kN for various soft clay interlayer thicknesses: (a) bending movements; (b) lateral pile deflections; (c) maximum bending moments; (d) pile head displacements